PROCEEDINGS OF SCIENCE

Status and prospects of LHCb

Andrei Golutvin* **CERN, Imperial College London, ITEP Moscow**

E-mail: andrey.golutvin@cern.ch

The status of the LHCb detector is presented. A particular emphasis is given to the LHCb strategy for New Physics searches in CP-violation and rare decay measurements. Prospects for early physics results are reviewed as well.

European Physical Society Europhysics Conference on High Energy Physics, EPS-HEP 2009,
July 16 - 22 2009
Krakow, Poland

*Speaker.

PoS(EPS-HEP 2009)025

1. LHCb detector and its expected performance

The LHCb detector, described in detail elsewhere [1], has been designed and constructed in order to search for new physics beyond the Standard Model (SM) at the Large Hadron Collider (LHC) via precision measurement of CP-violation and rare decays of heavy flavours. The main advantages of heavy flavours studies at hadron collider is the accessibility to all b-hadrons, in particular B_s mesons, which being boosted allow for the possibility of time-dependent studies, and a large $b\bar{b}$ production cross-section. The cross section of $b\bar{b}$ pairs produced in proton-proton collisions at $\sqrt{s} = 14$ TeV is expected to be $\sim 500\mu b$. A total of 10^{12} $b\bar{b}$ pairs are produced per year running at the nominal LHCb luminosity of 2×10^{32} cm^{-2} s^{-1}, which corresponds to an annual integrated luminosity of 2 fb^{-1}.

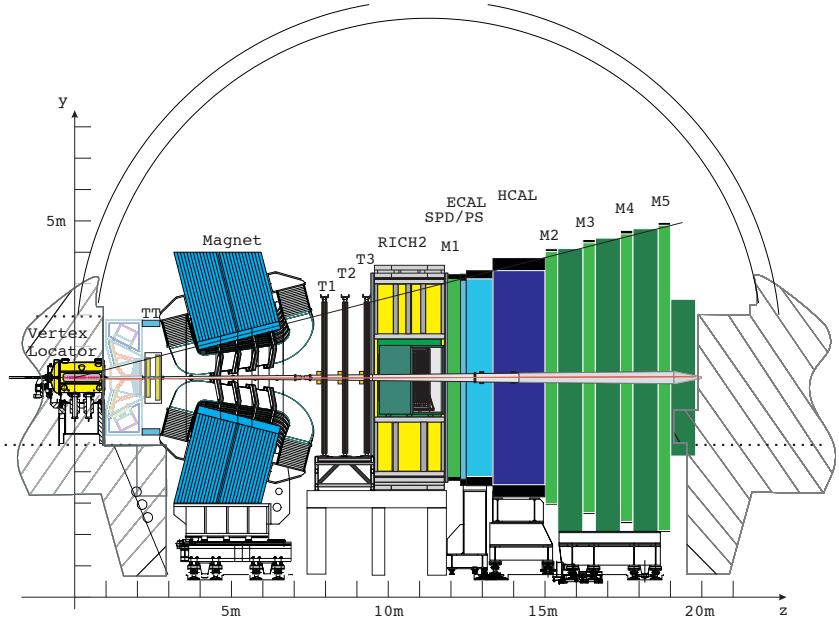

Figure 1: Schematic side view of the LHCb detector showing the following components: Vertex Locator (VELO), RICH1, Trigger Turicencis (TT), warm dipole magnet, three stations of the main tracker (T1,T2,T3), RICH2, Scintillating Pad Detector (SPD), PreShower (PS), Electromagnetic (ECAL) and Hadronic (HCAL) calorimeters and Muon detector stations (M1 - M5).

To maximize the detector acceptance for flavour physics LHCb has been constructed as a forward angle spectrometer with an angular coverage of $\sim$ 15 to 300(250) mrad in the bending (non-bending) plane. A side view of the LHCb detector is shown in Figure 1. The key features of LHCb are:

- Excellent vertexing capabilities and proper time resolution of $\sim$ 40 fs, as provided by the Vertex Locator (VELO), the detectors of which approach to within 8 mm of the beam line during collisions;
- Particle identification capabilities provided by two RICH detectors which allow for good π/K separation in 2 - 100 GeV/c momentum range;

- Good momentum resolution $\delta p/p \sim 0.3 - 0.5\%$ depending on p, which together with precise track direction measurement, results in excellent invariant mass resolution of $\sim$ 10 - 20 MeV/c^2 depending on the B decay channel;
- A selective and flexible trigger system.

High performance trigger operation is a crucial requirement for the success of the LHCb physics programme since the $b\bar{b}$ cross-section constitutes less than 1% of the total inelastic cross-section and the typical branching fractions of B decays of interest are less than $\sim 10^{-5}$. A schematic of the LHCb trigger implementation is shown in Figure 2.

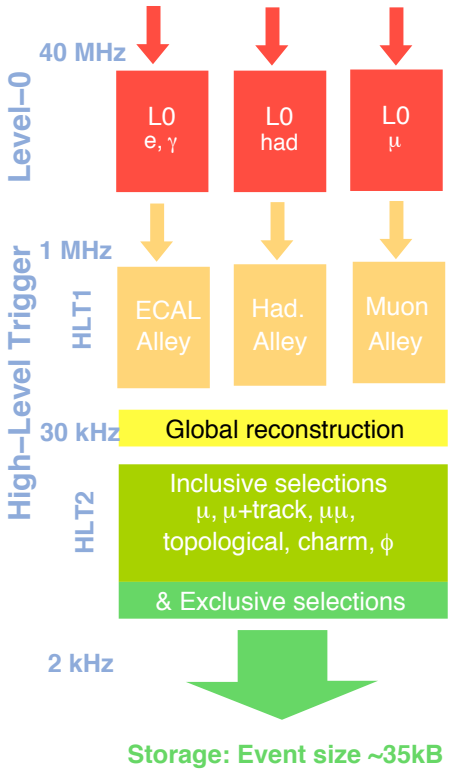

Figure 2: Conceptual diagram of the LHCb trigger

The trigger system is composed of two parts [2].The hardware Level-0 (L0) trigger is implemented in custom made electronics while a High Level Trigger (HLT) is a software based trigger, which currently runs on $\sim$ 4000 multi-core commercially available processors. In order to reduce the input rate down to $\sim$1 MHz, L0 searches for muon, electron, photon and hadron candidates with p_T significantly higher than in minimum bias events. The backwards planes of the VELO contribute as a Pile-up detector, identifying events with multiple interactions, which can then be rejected or triggered on with adjusted p_T thresholds. The HLT further reduces the rate down to $\sim$2 kHz by first confirming and refining the L0-candidates with more complete information on their impact parameter and lifetime, and then selecting partially or fully reconstructed B decay

modes. After HLT, selected events are written to storage at ∼2 kHz rate for subsequent off-line analysis.

1.1 Commissioning of LHCb detector

The LHCb detector has been successfully commissioned using cosmic rays and beam induced events. Although the horizontal configuration of LHCb is not well suited for measuring cosmic rays, several million cosmic events have been collected for the time and spatial alignment of large sub-systems, such as the calorimeter, muon and outer tracker. For the smaller area and fine granularity detectors, like Inner Tracker (IT), TT and VELO, LHC beam-induced events have been effectively utilized. Occasionally during the LHC injection tests the proton bunches from SPS were dumped onto a beam stopper located close to the LHC injection point and only about 340 m downstream of LHCb. The resulting high intensity flux of produced secondary particles, traveling almost parallel to the LHC beam line, have been reconstructed by the VELO, TT and IT sub-detectors. This data sample had a typical fluence of ~ 100 particles/cm^2 allowed a time alignment to be achieved with a precision better than 2 ns and to test *in situ* the alignment from metrology measurements. In particular, for the VELO detector the module alignment parameters have been found to be within 10 μm for translation and 200 μmrad for rotation with respect to their nominal position [3].

2. LHCb physics program

The main goal of LHCb physics programme is to search for the virtual contribution of New Particles (NP) to Flavour Changing Neutral Currents (FCNC) in reactions mediated by the loop diagrams involving beauty and charm quarks. A search strategy has been developed on an illustrative set of "key measurements" [4] sensitive to the phases and couplings of NP and even to their helicity structure. Loop mediated FCNC reactions described by box or penguin diagrams, shown in Figure 3, may have different sensitivity to various NP effects. Thus LHCb will search for NP effects in the box and penguin diagrams separately. In the following we summarize in Sections 2.1

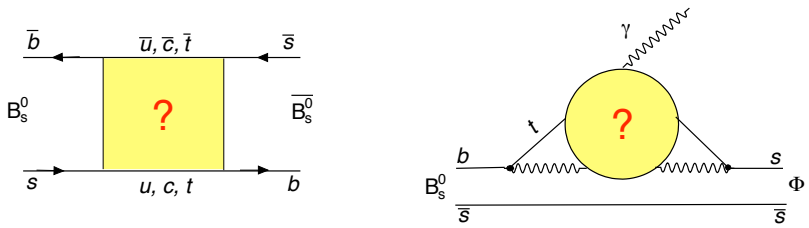

Figure 3: Box (left) and radiative penguin (right) diagrams. The internal lines may consist of either SM or new particles.

and 2.2 the status of some of the important observables in flavour physics, while in Section 2.3 we give the prospects for LHCb in this set of illustrative key measurements.

2.1 Measurements sensitive to the phases of NP

The most promising way to search for NP phases contributing to box diagrams is in the measurement of the B_s mixing phase ϕ_s. Within the SM this CP violating phase is predicted very accurately and expected to be very small: $\phi_s^{SM} = -2\beta_s = (0.0360^{+0.0020}_{-0.0016})$ [5]. Until now measurements have had low sensitivity to this observable, but recent results from the Tevatron hint at a value far larger than the SM prediction, $2\beta_s \in [0.54,\ 1.18] \cup [1.94,\ 2.60]$ @ 68% *CL* [6, 7, 8].

Alternatively NP contributions to box diagrams can be searched for making a consistency test of the main Unitarity Triangle (UT), shown in Figure 4. This test requires the measurement of all the elements of the main Unitarity Triangle (UT) meaning that the exercise is more involved and less straightforward to interpret. Currently the precision of the UT elements is limited for the two non-trivial sides, on account of the uncertainties of the lattice QCD inputs, and by experimental errors for the three angles. Thanks to the B factories the angle β has been measured to a precision better than $\sim 1^\circ$, $\beta = (21.65^{+0.91}_{-0.89})^\circ$) [5]. The accuracy of the other two angles, α and γ, is currently rather modest, in particular for γ, where the limited statistics lead to a $\sim 20^\circ$ uncertainty [5].

Two of the five UT elements, the side opposite to the angle β and the angle γ can be extracted from the measurement of the reactions explicitly described by tree diagrams, which are insensitive to NP. In contrast, the other two elements, the angle β and the side opposite to the angle γ, can potentially receive virtual contribution from NP to the box diagrams.

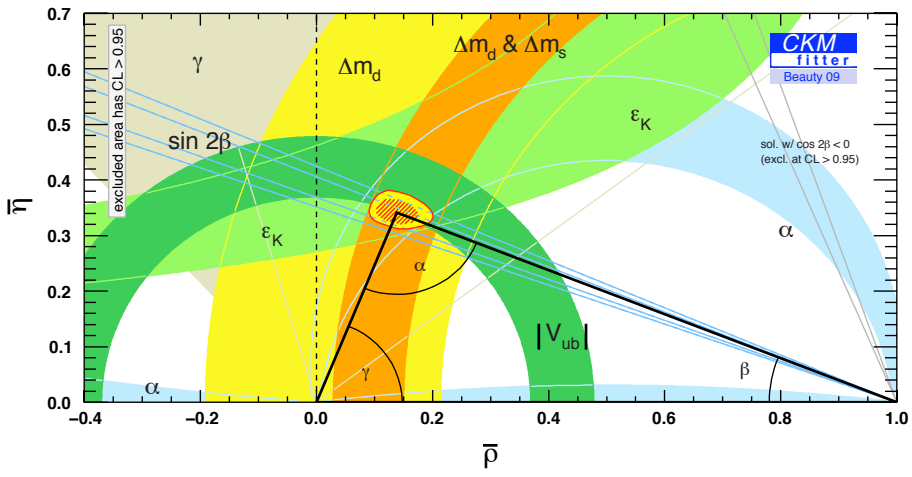

Figure 4: Constraints from the global CKM fir in the $(\bar{\rho}\,\bar{\eta})$ plane

Due to the specific shape of the UT, with the angle α being close to 90°, possible contributions from NP are mainly constrained by the comparison of the angles with the opposite sides, namely β with the side proportional to $\frac{|V_{ub}|}{|V_{cb}|}$ or γ with the side proportional to $\frac{|V_{td}|}{|V_{ts}|}$. As of today both tests suffer from rather limited accuracy. For the first pair of elements, the determination of the side is limited by $\sim 10\%$ accuracy of the $|V_{ub}|$ extraction methods [9] while for the second pair the statistical error of the angle γ measurement is by far the limiting factor. Indeed, the CKMFitter prediction for extracted from direct measurements, $\gamma = (73\pm^{22}_{25})^\circ$ [5], is significantly less accurate than the value following from the global SM constraint: $\gamma = (67.9\pm^{4.3}_{3.8})^\circ$ [5]. This SM constraint is

mainly based on the measurement of the processes mediated by the box diagrams, such as the angle β, which gives the phase of the B_d oscillation, and the side opposite to the angle γ side, which is proportional to the ratio of the B_d to B_s oscillation frequencies.

2.2 Measurements sensitive to NP couplings and their helicity structure

Rare loop-induced B decays offer a set of experimental observables sensitive to the masses and couplings of NP. Current experimental sensitivity is limited by the statistics of the available data samples leaving room for sizable effects caused by NP contribution.

Assuming a generic coupling the inclusive measurement of $BR(b \to s\gamma)$ indirectly constraints the scale of NP masses to $\Lambda > 10^3$ TeV [10]. NP models with specific couplings can be effectively tested using exclusive rare B decays. The often cited example is the super-rare $B_s \to \mu^+\mu^-$ decay. In the SM this helicity suppressed decay has a branching ratio of $BR(B_s \to \mu^+\mu^-) = (3.35 \pm 0.32) \times 10^{-9}$ [11]. In the MSSM with an extended Higgs sector $BR(B_s \to \mu^+\mu^-)$ is proportional to $\frac{tan^6\beta}{M_A^4}$ [12] and so may significantly exceed the SM prediction for large values of the $tan\beta$ parameter. The best current limit from CDF, $BR(B_s \to \mu^+\mu^-) < 4.3 \times 10^{-8}$ @ 90% CL [13], is still an order of magnitude higher that the SM prediction.

Several strategies have been proposed to search for NP effects in the processes mediated by radiative and electroweak penguin diagrams through the measurement of the helicity structure of the inherent amplitudes. Owing to the $V-A$ structure of the W-boson coupling, the photon produced in $b \to s\gamma$ transition is predominantly left-handed up to corrections of order $\frac{m_s}{m_b}$, which arise from a chirality flip. A contribution of soft gluons to the penguin loop may further increase the fraction of right-handed photons; recent calculation [14] predict a $\sim 1\%$ increase.

The fraction of right-handed photons produced in $b \to s\gamma$ transition can be extracted from the measurement of the time-dependent CP-asymmetry in exclusive $B_s \to \phi\gamma$ decays (the corresponding diagram is shown in Figure 3). In general, the time-dependent rate of $B_s(\bar{B}_s)$ mesons decaying to a photon and the CP-eigenstate f^{CP} is given by:

$$\Gamma(B_s(\bar{B}_s)) \propto e^{-\Gamma_s t}\{\cosh\frac{\Delta\Gamma_s t}{2} - \mathscr{A}^{\Delta}\sinh\frac{\Delta\Gamma_s t}{2} \pm C\cos\Delta m_s t \mp S\sin\Delta m_s t\}.$$

Following the notations of [15, 16] in the SM $S \approx \sin 2\psi \sin\phi_s$, $\mathscr{A}^{\Delta} \approx \sin 2\psi\cos\phi_s$ and $C \approx 0$, where $\tan\psi \equiv |\frac{A(\bar{B}\to f^{CP}\gamma_R)}{A(B\to f^{CP}\gamma_L)}|$ is related to the fraction of the photons with "wrong" helicity. Since $\cos\phi_s \sim 1$ in the SM, a measurement of $\mathscr{A}^{\Delta}$ through the study of time-dependent rates of $B_s(\bar{B}_s) \to \phi\gamma$ provides a sensitive test of the $V-A$ structure of weak interactions in FCNC processes.

As shown in Figure 5, the decay $\bar{B}_d \to \bar{K}^{*0}\mu^+\mu^-$ proceeds via a combination of the electroweak penguin and box diagrams. The FCNC describing this $b \to s$ transition contains a right-handed component that is well calculable in the SM but can be affected by NP contributions resulting in modified angular distributions. As an example, the forward-backward asymmetry, $A^{FB}(q^2 = m^2_{\mu\mu})$ [17, 18], is particularly sensitive to NP contributions at its zero-point, s_0, since the dominant theoretical uncertainty from hadronic form-factors cancels out at leading order.

At low values of q^2 the decay $\bar{B}_d \to K^{*0}e^+e^-$ is dominated by the contribution from the virtual photon and therefore is very sensitive to the photon helicity providing a complementary measurement to the time-dependent CP violation measurement in $B_s \to \phi\gamma$ decays.

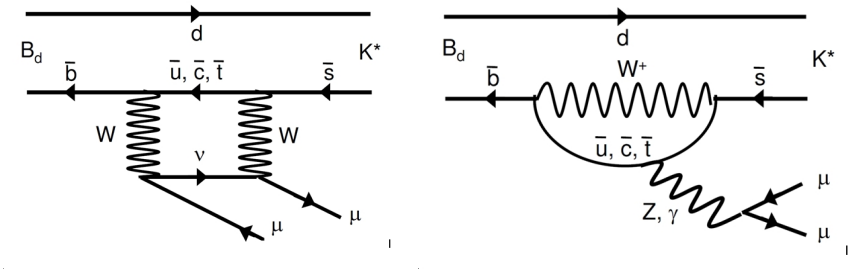

Figure 5: Box (left) and electroweak penguin (right) diagrams describing $\bar{B}_d \to K^* \mu^+ \mu^-$ decay

2.3 LHCb performance for the key measurements

Key measurements	Accuracy in 1 nominal year ($2 fb^{-1}$)
β_s	0.03
γ in trees	4.5°
γ in loops	7°
$B_s \to \mu\mu$	3σ measurement down to SM prediction
$B \to K^* \mu\mu$	$\sigma(s_0) = 0.5\ GeV^2$
Polarization of photon in radiative penguin decays	$\sigma(H_R/H_L) = 0.1$(in $B_s \to \phi\gamma$) $\sigma(H_R/H_L) = 0.1$(in $B_d \to K^* e^+ e^-$)

Table 1: Expected LHCb sensitivities for the key measurements, achieved with the data sample of 2 fb[1] integrated luminosity.

The LHCb key measurements include:

- A measurement of the B_s mixing phase ϕ_s in $B_s^0 \to J/\psi(\mu\mu)\phi(KK)$ decays [19];
- A measurement of the UT angle γ in the processes mediated by tree diagrams [20], further referred to as γ *in trees*, using both CP-violation time-integrated and time-dependent measurements. These include studies of decays of the type $B_u \to D^0 K^+$, $B_d \to D^0 K^{*0}$, $B_d \to D\pi$ and $B_s \to D_s K$;
- A measurement of the UT angle γ in loop mediated processes [20], further referred to as γ *in loops*. The $B^0_{d,s} \to h^+ h^-$ family of decays, where h stands for a pion or kaon, have decay rates with sizable contribution from penguin diagrams, making them sensitive to NP effects in penguin loops. Allowing for a 20% U-spin symmetry breaking, the UT angle γ can be extracted with a precision of 7° after one nominal LHCb year of data taking;
- A measurement of the super-rare $B_s \to \mu^+ \mu^-$ decay [21];
- A test of the $V-A$ helicity structure of the weak interaction in loop mediated $B_s \to \phi\gamma$ and $B_d \to K^{*0} \ell^+ \ell^-$ decays, where ℓ stands for an electron or muon [21].

The LHCb performance for the key measurements is described in detail in [4]. Expected sensitivities, achieved with the data sample of 2 fb^{-1} integrated luminosity, are summarized in Table 1.

3. Prospects for physics in 2010

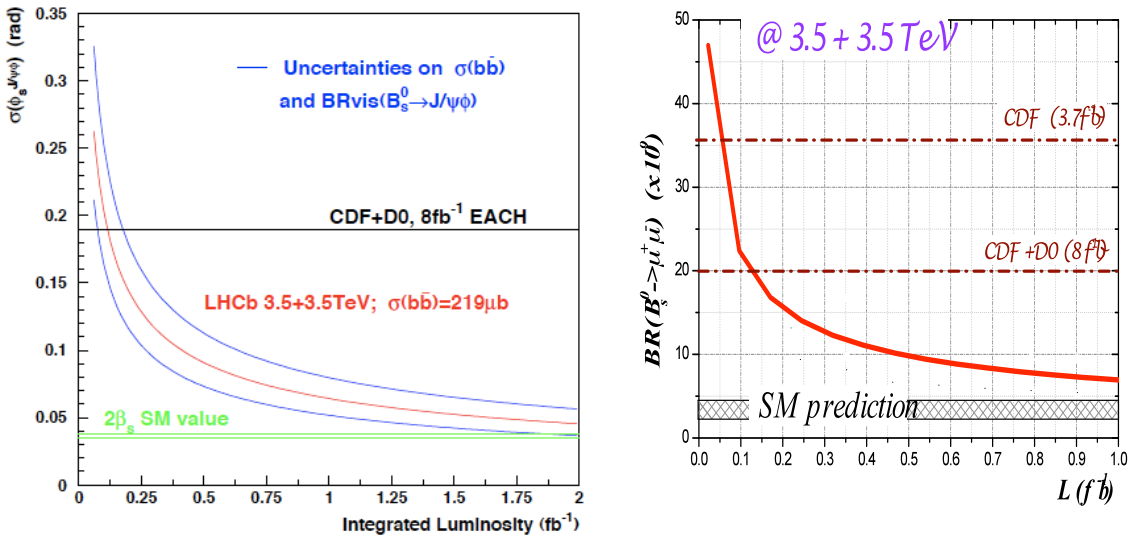

Figure 6: Left: Statistical uncertainty for the ϕ_s measurement as a function of the integrated luminosity. The outer lines indicate the uncertainties coming from the $b\bar{b}$ cross-section and visible branching ratio of $B_s \to J/\psi(\mu\mu)\phi(KK)$. Right: Exclusion limit for BR($B_s \to \mu^+\mu^-$) at 90% CL as a function of the integrated luminosity.

The current LHC plan foresees the two years physics run at the center-of-mass-energy of 7 TeV in order to collect the data sample of ~ 1 fb^{-1} integrated luminosity, of which ~ 200 pb^{-1} should be available for physics analysis already in 2010.

LHCb plans for early physics studies will evolve in accordance to the integrated luminosity delivered by LHC. Apart from using first data for an understanding of the track reconstruction and particle identification, inclusive V0 production will be studied, followed by the measurement of differential cross-section for the prompt J/ψ production as well as the $b\bar{b}$ production cross-section. High class measurements in the charm sector are feasible with ~ 200 pb^{-1} integrated luminosity. For example, LHCb expects to collect a data sample of $\sim 10^7$ flavour tagged $D^0 \to KK$ events that should improve significantly the sensitivity of D mixing and CP-violation studies compared to existing the B factories results.

With 200 pb^{-1} integrated luminosity LHCb, even when running at the reduced centre-of-mass-energy of $\sqrt{s} = 7$ TeV, has an excellent opportunity to improve on the Tevatron sensitivity in several key measurements in the beauty sector. Figure 6 for example show LHCb prospects for the measurement of the phase ϕ_s and the search for the mode $B_s \to \mu^+\mu^-$ with integrated luminosity.

References

[1] B. Adeva *et al.,* (LHCb Collaboration) *"The LHCb Detector at LHC,"* JINST (2008) 3 508005.

[2] K. Vervink, these proceedings.

[3] T. Bowcock, these proceedings.

[4] B. Adeva *et al.,* (LHCb Collaboration) *"Roadmap for selected key measurements of LHCb,"* arXiv:0912.4179 [hep-ex].

[5] CKMfitter Group (J. Charles et al.), Eur. Phys. J. C41, 1-131 (2005) [hep-ph/0406184].

[6] T. Aaltonen *et al.* [CDF Collaboration], "First Flavor-Tagged Determination of Bounds on Mixing-Induced CP Violation in $B_s^0 \to J/\psi\phi$ Decays," Phys. Rev. Lett. **100** (2008) 161802 [arXiv:0712.2397 [hep-ex]]; CDF collaboration, "An updated measurement of the CP violating phase $\phi_s^{J/\psi\phi}$", CDF/ANAL/BOTTOM/PUBLIC/9458 (2008);

[7] V. M. Abazov *et al.* [D0 Collaboration], Phys. Rev. Lett. **101** (2008) 241801 [arXiv:0802.2255 [hep-ex]].

[8] CDF and D0 collaboration, "Combination of D0 and CDF results on $\Delta\Gamma_s$ and the CP-violationg phase $\beta_s^{J/\psi\phi}$", CDF/PHYS/BOTTOM/CDFR 9787, DÃŸ note 59-28-CONF (2009).

[9] C. Amsler *et al.* [Particle Data Group], Phys. Lett. B **667** (2008) 1., and 2009 partial update for the 2010 edition.

[10] Y. Nir, Nucl. Phys. Proc. Suppl. **117** (2003) 111 [arXiv:hep-ph/0208080].; S. Y. Nir Talk at the 2008 European School of High-Energy Physics, Herbeumontsur- Semois, Belgium, 8-21 June 2008.

[11] M. Blanke, A. J. Buras, D. Guadagnoli and C. Tarantino, JHEP **0610** (2006) 003 [arXiv:hep-ph/0604057].

[12] S. R. Choudhury and N. Gaur, Phys. Lett. B **451** (1999) 86 [arXiv:hep-ph/9810307]. C. S. Huang, W. Liao, Q. S. Yan and S. H. Zhu, Phys. Rev. D **63** (2001) 114021 [Erratum-ibid. D **64** (2001) 059902] [arXiv:hep-ph/0006250]. P. H. Chankowski and L. Slawianowska, Phys. Rev. D **63** (2001) 054012 [arXiv:hep-ph/0008046]. K. S. Babu and C. F. Kolda, Phys. Rev. Lett. **84** (2000) 228 [arXiv:hep-ph/9909476]. C. Bobeth, T. Ewerth, F. Kruger and J. Urban, Phys. Rev. D **64** (2001) 074014 [arXiv:hep-ph/0104284].

[13] CDF Collaboration, T. Aaltonen *et. al.,* (CDF Collaboration), Phys. Rev. Lett. 100 (2008) 101802 [0712.1708]; *"Search for $B_s^0 \to \mu^+\mu^-$ and $B_d^0 \to \mu^+\mu^-$ decays with $3.7 fb^{-1}$ of $p\bar{p}$ collisions with CDF II."* CDF Public Note 9892, 2009.

[14] P. Ball and R. Zwicky, Phys. Lett. B **642** (2006) 478 [arXiv:hep-ph/0609037].

[15] D. Atwood, M. Gronau and A. Soni, Phys. Rev. Lett. 79 (1997) 185 [arXiv:hep-ph/9704272].

[16] D. Atwood, T. Gershon, M. Hazumi and A. Soni, Phys. Rev. D 71 (2005) 076003 [arXiv:hep-ph/0410036].

[17] A. Ali, P. Ball, L. T. Handoko and G. Hiller, Phys. Rev. D **61** (2000) 074024 [arXiv:hep-ph/9910221].

[18] M. Beneke, T. Feldmann and D. Seidel, Nucl. Phys. B **612** (2001) 25 [arXiv:hep-ph/0106067].

[19] M. Calvi, these proceedings.

[20] M. Gersabeck, these proceedings.

[21] M.-H. Schune, these proceedings.